

# **Characterization of Multi-layered Porous Components of Batteries and Fuel Cells**

Akshaya Jena and Krishna Gupta  
Porous Materials, Inc.  
83 Brown Road, Ithaca, NY 14850

## **Abstract**

Determination of porosity of individual layers of composites is not possible by the available techniques. A novel technique that can be used to measure such porosity is described. In this technique, the sample is soaked in a wetting liquid. The wet sample is loaded in the specially designed instrument. Measured pressure and flow rates are used to compute constricted pore diameter, the largest pore diameter, the mean flow pore diameter and the pore size distribution of individual layers. The component containing two layers was examined using the new technique and porosimetry. The new technique successfully performed the pore structure analysis of the two layers of the composite.

## **1. Introduction**

Multi-layered composite sheets of porous materials are currently being used in batteries and fuel cells for improving their performance. Determination of pore characteristics of individual layers of composites is vital for design and applications. Mercury intrusion technique is normally used for pore analysis. However, it is often difficult to determine the porosity of individual layers. Flow porometry measures flow through the sheet material and can determine the structure of one layer. A novel technique has been developed to measure the pore structure of each layer of the composite sheet material. The technique has been described. Results of experiments with a two-layer composite using the new technique and porosimetry have been presented. The pore structures of the two layers could not be determined by porosimetry, but could be determined by the new technique.

## **2. Technique**

### **2.1. Material**

The component investigated was a composite consisting of two layers. One of the layers had very small pores while the other had large pores. The composite is sketched in Figure 1. The layer with small pores is designated top layer, while the layer with large pores is designated bottom layer.

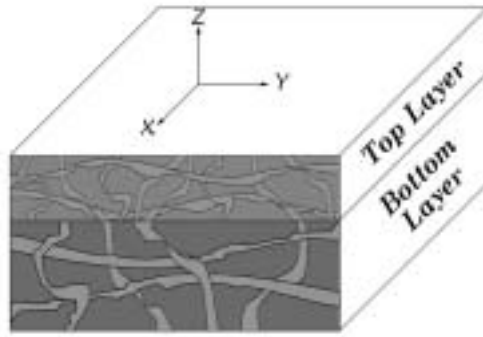


Figure 1. Sketch of the two-layer composite.

## 2.2. Flow Porometry

This is a novel technique that uses wetting liquids to fill the pores in the sample. The solid/liquid surface free energy of a wetting liquid is lower than the solid/gas surface free energy. Therefore, filling of pores occurs spontaneously, but a non-reactive gas under pressure is required to force the liquid out of the pores. The pressure required to displace the liquid at any location in the pore can be obtained by equating the work done by the gas to the increase in surface free energy [1].

$$p = (\gamma \cos \theta) (dS / dV) \quad (1)$$

$p$  = differential gas pressure on the liquid in the pore

$\gamma$  = surface tension of liquid

$\theta$  = contact angle

$dV$  = incremental volume of gas in the pore

$dS$  = incremental solid/gas surface area due to  $dV$ .

$(dS / dV)$  is a measure of pore size. The diameter  $D$  at a given location in the pore is defined as diameter of a cylindrical opening such that:

$$(dS / dV)_{\text{pore}} = (dS / dV)_{\text{opening}} \quad (2)$$

The  $(dS / dV)$  of a cylindrical pore of diameter  $D$  is  $(4/D)$ . Substituting in Equation 1:

$$D = (4 \gamma \cos \theta) / p \quad (3)$$

It has been shown that  $\cos \theta$  is close to one for wetting liquids with low surface tension [2]. For low surface tension liquids:

$$D = 4 \gamma / p \quad (4)$$

Pore characteristics are computed from measured pressures and gas flow rates.

The completely automated instrument that contained state-of-the-art components and innovative design features, and yielded reproducible and accurate data [3] is shown in Figure 2.



Figure 2. The Capillary Flow Porometer.

The sample chambers of the flow meter were specially designed. The chamber shown in Figure 3 holds the sample between two o-rings so that gas flows through pores in the thickness direction (z-direction) of the sample (Figure 1). In the chamber shown in Figure 4, the sample is held between two non-porous plates. The plate below the sample has a small circular opening to allow access of the gas to the sample. The gas flows in directions parallel to the plane (x & y directions) of the sample (Figure 1).

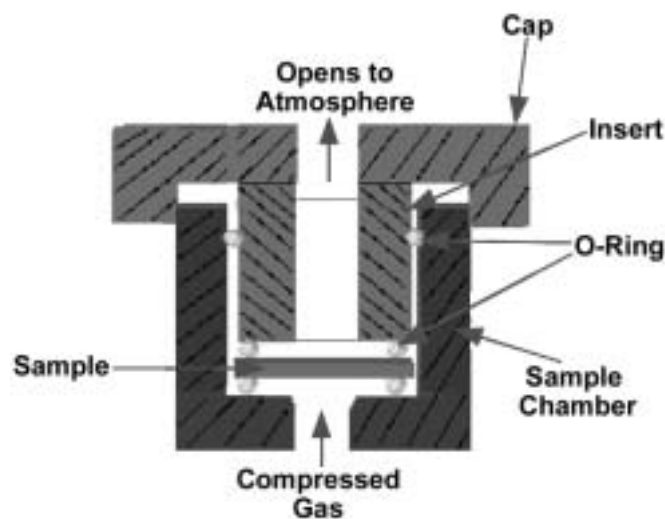


Figure 3. Sample chamber for flow along z-direction.

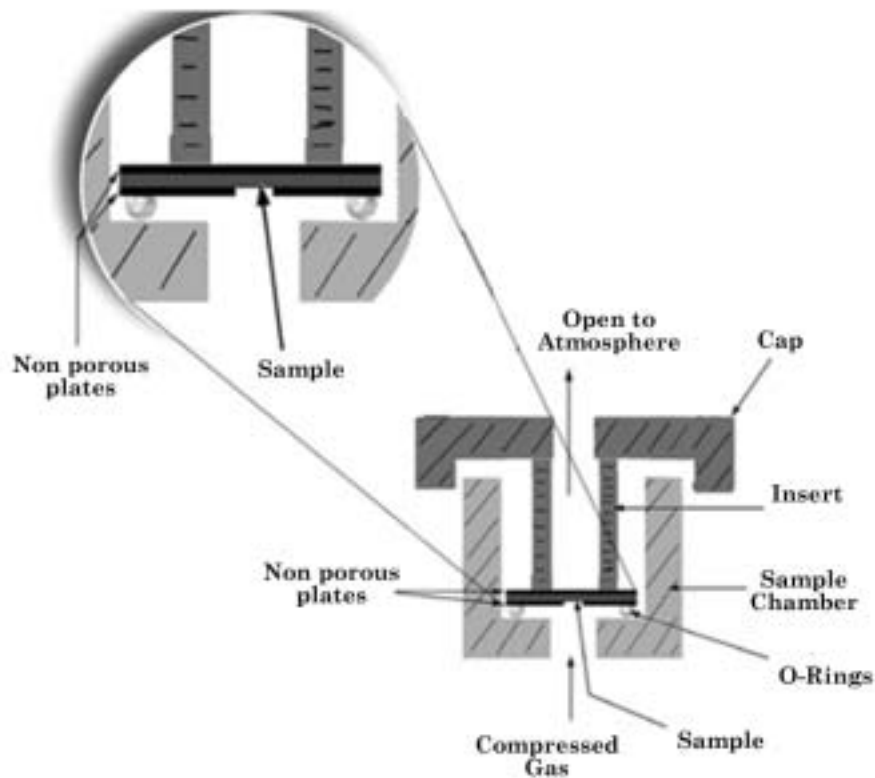


Figure 4. Sample chamber for flow along x & y directions.

The wetting liquid galwick was used. Its surface tension was 15.9 dynes/cm and  $\cos \theta$  was taken as one. Air pressure under the bottom layer was increased to displace the liquid in pores.

### 2.3. Mercury Intrusion Porosimetry

Mercury is non-wetting to most solids because the solid/liquid surface free energy is greater than the solid/gas surface free energy. Mercury cannot flow spontaneously into pores, but under pressure, mercury can be forced into pores. The pore volume is the volume of the intruded liquid and pore size is related to pressure. Using the procedure used for derivation of relations for flow porometry, it can be shown that:

$$D = - (4 \gamma \cos \theta) / p \quad (5)$$

$p$  = intrusion pressure

$\gamma$  = surface tension of intrusion liquid

$\theta$  = contact angle

Measured intrusion volume and pressure were used to compute pore size, pore volume and pore volume distribution. The surface tension and contact angles of mercury used in the calculations were 480 dynes/cm and  $140^\circ$  respectively.

### 3. Results and Discussion

#### 3.1. Flow Porometry

##### 3.1.1. Pore diameters of the top layer

Equation 4 relates measured pressure at which gas flows through a pore, to the pore diameter. The pore diameter varies along the path of the pore (Figure 5) and consequently, the pressure required to displace the liquid also varies along the path of the pore. The pressure has its maximum value at the most constricted part of the pore (Figure 5). Therefore, only when the maximum pressure is reached, gas completely empties the pore and flows through the pore to increase the flow rate at the applied pressure. The pore diameter computed from pressure measured in flow porometry is the diameter at the most constricted part of the pore.

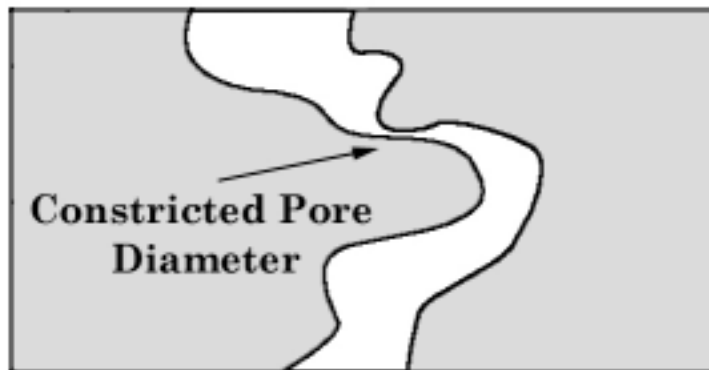


Figure 5. Variation of pore diameter along the path of the pore.

In the two-layer composite sample, gas flowing in the z-direction must flow first through pores in the bottom layer and then through pores in the top layer. Because pores in the bottom layer are much larger than those in the top layer, pores in the top layer act as constrictions. Therefore, pore diameters measured by flow porometry are the diameters of constricted parts of pores in the top layer.

Flow rate versus pressure plots obtained using wet and dry samples [4], are presented in Figure 6. It follows from Equation 4 that the pressure at which flow starts corresponds to the opening of the largest pore. This pressure is known as the bubble point pressure. The largest pore diameter computed using the bubble point pressure is 2.214  $\mu\text{m}$  in the top layer.

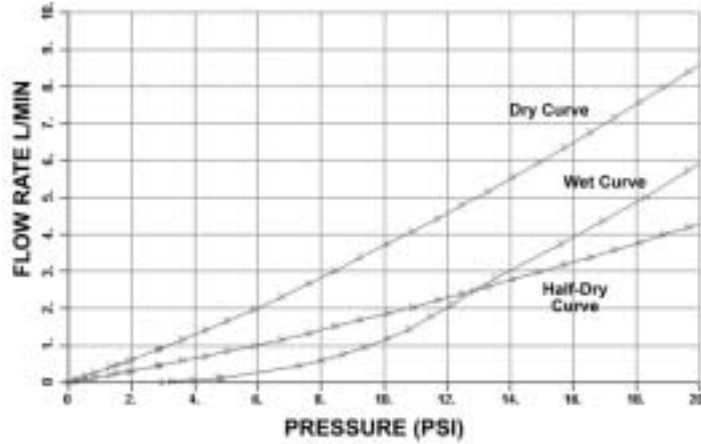


Figure 6. Variation of flow rate with pressure for flow in the z-direction.

The half-dry curve in Figure 6 is computed from the dry curve and gives half of the flow rate through the dry sample at a given differential pressure. Pressure at the intersection of the half-dry curve with the wet curve is the mean flow pressure (Figure 6), which is used to calculate the mean flow pore diameter. The mean pore diameter in the top layer is  $0.514 \mu\text{m}$ . Half of the flow through the sample is through pores larger than the mean pore.

The dry curve in Figure 6 gives flow rate through the composite in the z-direction. These data are used to calculate permeability of air through the composite. Permeability of any fluid through the composite sample can be evaluated by generating the flow versus pressure curve using a dry sample.

### 3.1.2. Pore distribution in the top layer

The following equation defines the pore distribution function:

$$f = - d[100 \times (F_w / F_d)] / dD \quad (6)$$

where,  $F_w$  and  $F_d$  are the flow rates through wet and dry samples respectively at the same differential pressure. The distribution function of pores in the top layer was calculated from data in Figure 6 and is presented in Figure 7. It follows from Equation 6 that the area under the curve in Figure 6 in a given pore size range yields percent flow in that size range. The majority of pores are in the diameter range of about  $0.1 - 1 \mu\text{m}$ .

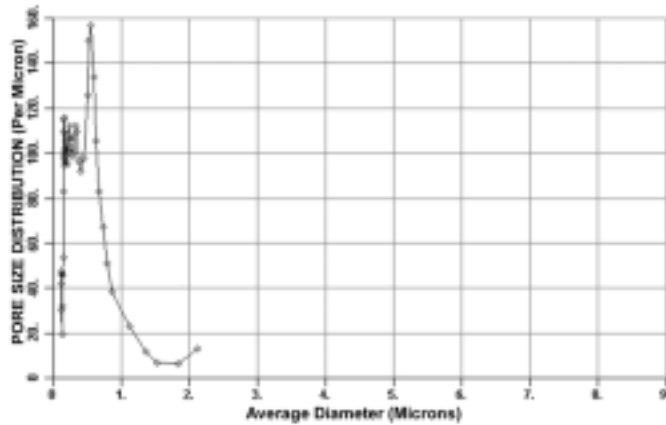


Figure 7. Pore distribution function in the top layer.

### 3.1.3. Pore diameter in the bottom layer

In experiments using the sample chamber shown in Figure 4, air entered the sample from below the bottom layer. Because pores in the bottom layer are larger than the pores in the top layer, pressure necessary for air to displace the liquid in the pores of the bottom layer is less than that of the top layer. Therefore, air displaced the liquid from pores in the bottom layer at a low pressure, flowed radially and escaped to the atmosphere. When the gas pressure became high, air also displaced liquid in the small pores of the top layer, moved radially and escaped to the atmosphere. Therefore, the largest pore diameter measured by this technique is the largest constricted pore diameter of pores in the bottom layer. However, the mean pore diameter is the average of all pores measured by this technique.

The change of flow rate with differential pressure for flow in the x & y directions [4] are shown in Figure 8. From the bubble point pressure and mean flow pressure the largest pore diameter and the mean flow pore diameter are computed as 11.57  $\mu\text{m}$  and 1.72  $\mu\text{m}$  respectively.

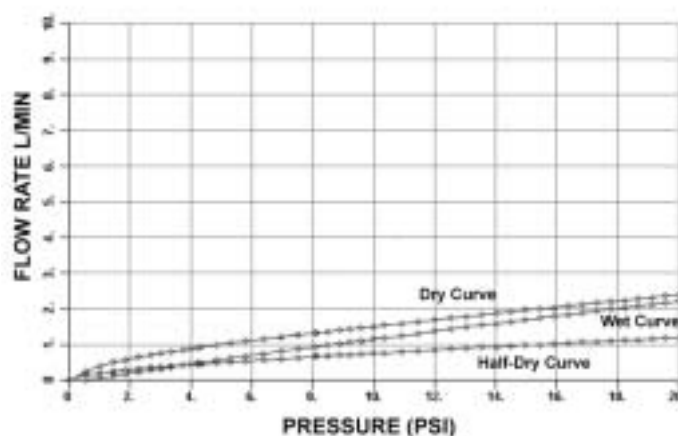


Figure 8. Variation of flow rate with pressure for flow in the x & y directions.

### 3.1.4. Pore distribution in the bottom layer

The pore distribution function calculated from data in Figure 8 are presented in Figure 9. The distribution function shows that the sample has two groups of pores. A large group of pores in the range of about 2-11.5  $\mu\text{m}$  and a small group of pores in the range of about 0.2 –1.5  $\mu\text{m}$ . The small group of pores are identical with the group of pores found in the top layer (Figure 9). Hence, the small group of pores detected by flow in the x & y directions is the group of pores of the top layer detected in the experiments with flow in the z-direction. The large group of pores is of the bottom layer.

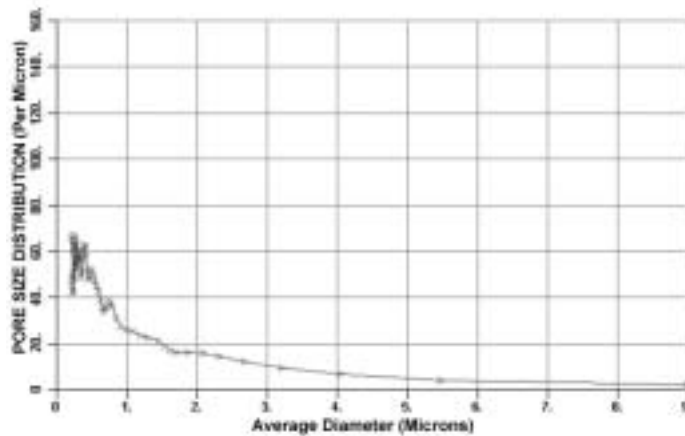


Figure 9. Pore size distribution from experiments with flow in the x & y directions.

## 3.2. Mercury Intrusion porosimetry

### 3.2.1. Pore volume

Intrusion volume of mercury measured as a function of pressure is shown in Figure 10. The plot shows the total volume of pores in the two layers. Although there are two inflection points in the curve, it is not possible to separate the pore volume of one layer from the other.

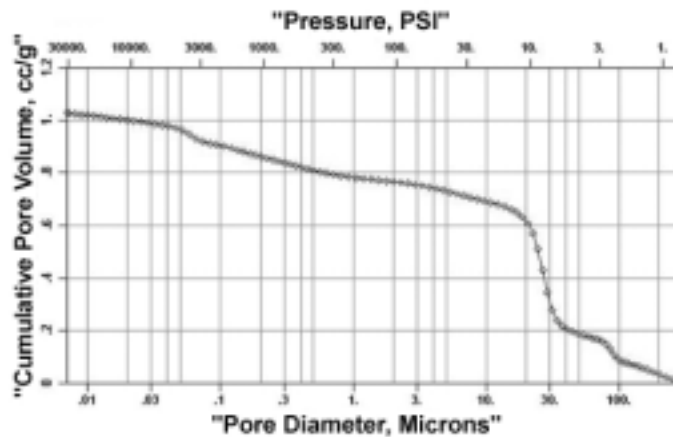


Figure 10. Pore volume of the composite by porosimetry

### 3.2.2. Pore volume distribution

The pore volume distribution computed from data in Figure 10 are presented in Figure 11. The plot shows one major peak at about 30  $\mu\text{m}$ , although the top and bottom layers of the composite have pores in the size ranges of 0.2-1.5  $\mu\text{m}$  and 2-11  $\mu\text{m}$  respectively. Porosimetry does not show the two groups of pores in the two layers. It is possible that the pore volume associated with the small pores of the top layer are too small to be detected by porosimetry.

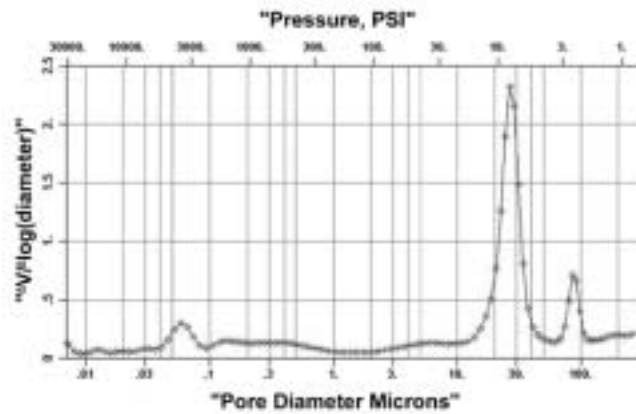
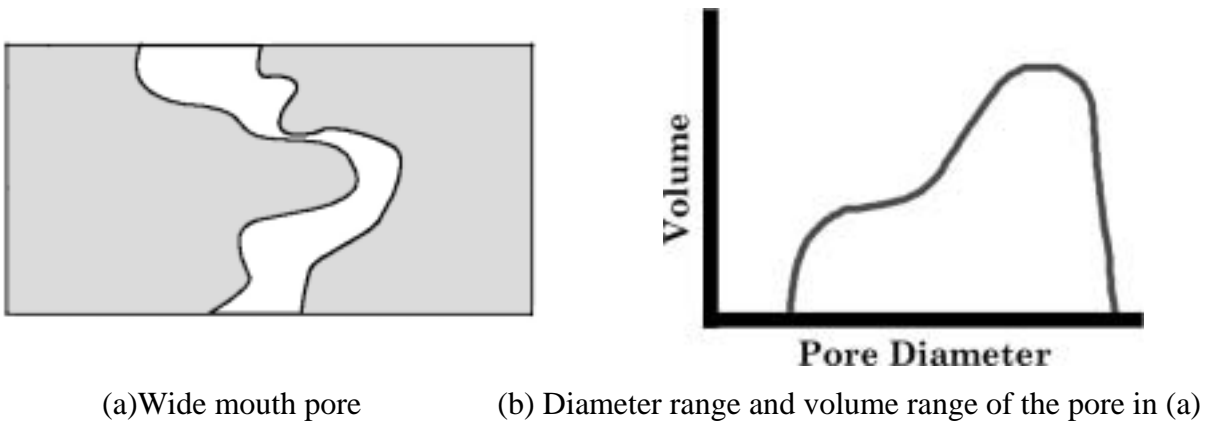


Figure 11. Pore volume distribution of the composite by porosimetry.

The large pore volume at large pore diameter was detected by porosimetry. This is because of the presence of wide mouth pores. A wide mouth pore is shown in Figure 13. Equation 5 suggests that wider parts of the pore will be filled at low pressures, while constricted parts of the pore will be filled at high pressure. Thus, a range of pore diameters and a range of pore volume of the same pore will be observed. There is no unique pore diameter value associated with a single pore.



(a) Wide mouth pore

(b) Diameter range and volume range of the pore in (a)

Figure 12. Detection of wide mouth pore by porosimetry

### **3.3. Comparison of Flow porometry and mercury porosimetry**

Flow porometry made it possible to measure constricted pore diameter, the largest pore diameter and pore size distribution of each layer of the two constituent layers of the composite. Porosimetry could not measure these characteristics. Pore volume and pore volume distribution of the individual layers of the composite could not be measured by porosimetry, although these characteristics of the composite as a whole could be measured. Also porosimetry involved use of toxic mercury and high pressures, which is likely to modify the pore structures of the layers.

### **4. Conclusions**

- (1) The pore structure of a battery component consisting of a two-layer composite was investigated using a novel technique based on flow porometry and porosimetry.
- (2) Porometry gave constricted pore diameter, the largest pore diameter, mean pore diameter and pore size distribution of each layer of the composite.
- (3) Porosimetry only gave the pore volume and pore volume distribution of the whole composite. None of the characteristics of individual layers could be determined.
- (4) Data obtained with the porometer could be used to evaluate permeability of the composite. It is not possible to measure permeability by porosimetry.
- (5) Porometry did not use toxic mercury or high pressure, which is likely to damage the pore structure. Porosimetry required the use of mercury and high pressure.
- (6) The novel technique based on flow porometry is suitable for pore structure analysis of constituent layers of a composite.

### References

1. A.K. Jena and K.M. Gupta, *Journal of Power Sources*, 80, 1&2, 46-52 (1999).
2. Vibhor Gupta and A.K. Jena, *Advances in Filtration and Separation Technology*, 13b, 833-44 (1999).
3. Vibhor Gupta and A.K. Jena, *Filtration News*, 17, 2, March/April (1999).
4. Akshaya Jena and Krishna Gupta, *Journal of Power Sources*, in press (2001).